Ciliberti *et al.*
Biotechnology for Biofuels and Bioproducts (2025) 18:65
https://doi.org/10.1186/s13068-025-02668-9

Biotechnology for Biofuels and Bioproducts

RESEARCH

Open Access

Enhancing selective itaconic acid synthesis in *Yarrowia lipolytica* through targeted metabolite transport reprogramming

Cosetta Ciliberti[1,6], Zbigniew Lazar[2], Kacper Szymański[2], Evgeniya Yuzbasheva[3], Tigran Yuzbashev[4], Ivan Laptev[5], Luigi Palmieri[1,6], Isabella Pisano[1,6] and Gennaro Agrimi[1,6*]

Abstract

Background Itaconic acid is a valuable platform chemical with applications in polymer synthesis and other industrial sectors. Microbial fermentation offers a sustainable production route, involving two fungi such as *Aspergillus terreus* and *Ustilago maydis*. However, their employment in industrial bioprocesses for itaconic acid production is characterized by several challenges. *Yarrowia lipolytica* is a non-conventional yeast that shows suitability for industrial production and it is widely employed as heterologous host to obtain relevant metabolites. This study aimed to engineer *Y. lipolytica* for the selective production of itaconic acid by optimising intracellular metabolic fluxes and transport mechanisms.

Results A metabolic engineering strategy was developed to prevent the secretion of citric and isocitric acids by blocking their transport at both mitochondrial and plasma membrane levels in *Y. lipolytica* strains. Specifically, the inactivation of *YlYHM2* and *YlCEX1* genes reduced secretion of citric and isocitric acid, enabling their accumulation in the mitochondria. Additionally, heterologous transporters from *Aspergillus terreus* (mttA and mfsA) and *Ustilago maydis* (mtt1 and itp1) were introduced to enhance the mitochondrial export of *cis*-aconitate and the extracellular secretion of itaconic acid. For the first time, complete gene set of the itaconate biosynthetic pathways from both fungal species were functionally expressed and compared in a yeast system with a similar genetic background. A synergistic increase in itaconic acid production was observed when both pathways were co-expressed, combined with the inactivation of native citric and isocitric transport. In contrast to previously engineered *Y. lipolytica* strains for itaconic acid production, the optimised strain obtained in this study does not require complex or nutrient-rich media, while achieving the highest product yield (0.343 mol IA/mol glucose) and productivity (0.256 g/L/h) reported in yeast, with minimal by-product formation.

Conclusions By integrating transporter engineering and pathway diversification, this study demonstrates an effective strategy to enhance itaconic acid production in *Y. lipolytica* while minimising by-product formation. The findings provide new insights into organic acid transport in yeast and open avenues for further optimization of microbial cell factories for sustainable biochemical production.

Keywords *Yarrowia lipolytica*, Itaconic acid, Transporters, Pathway diversification

*Correspondence:
Gennaro Agrimi
gennaro.agrimi@uniba.it
Full list of author information is available at the end of the article

Graphical Abstract

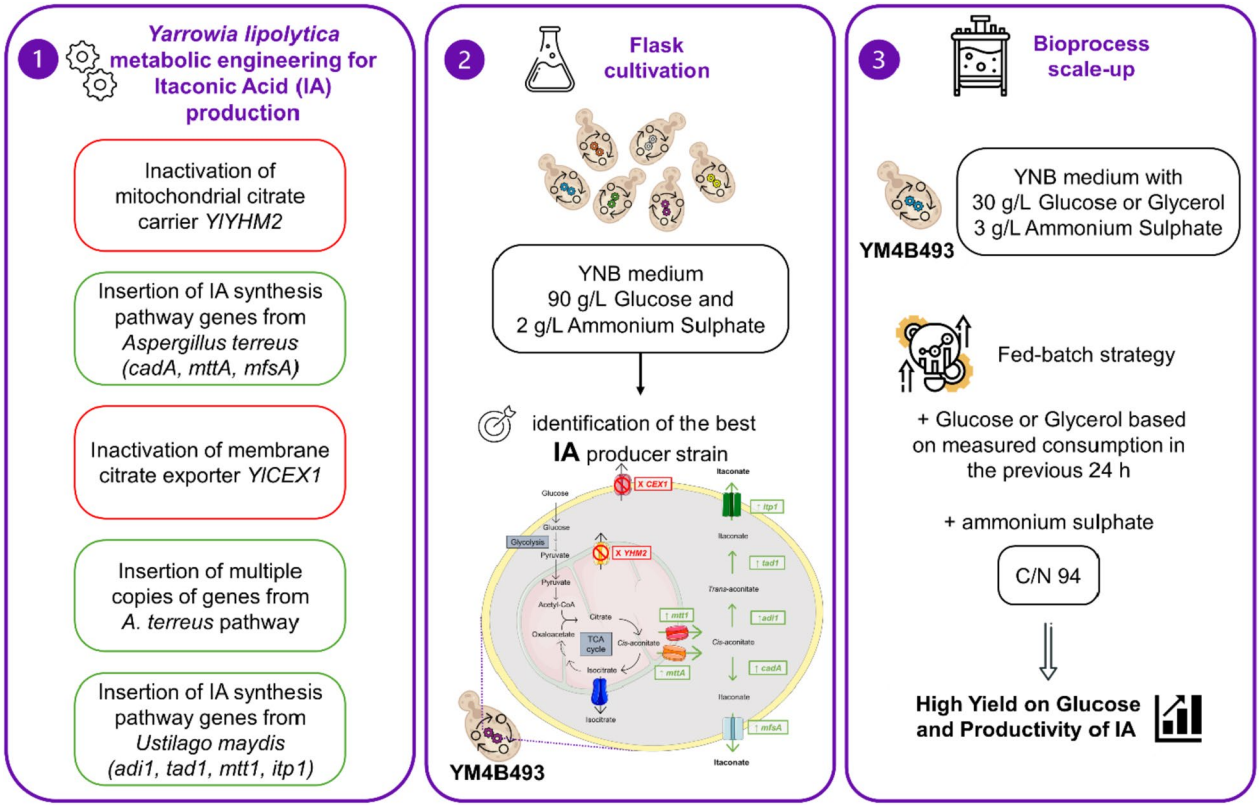

Background

Itaconic acid (IA), also called methylidenesuccinic acid, is an unsaturated dicarboxylic acid with the chemical formula $C_5H_6O_4$. Its distinctive chemical properties, including α,β-unsaturated functionality and two carboxylic groups, make it a valuable monomer in the chemical industry [1, 2]. IA has been inserted in the 12 value-added platform chemicals derived from biomass list by the U.S. Department of Energy [3] and its market value was estimated to reach 177.79 Million dollars by 2031, growing at a Compound Annual Growth Rate (CAGR) of 6.80% in the next seven years [4, 5]. IA is utilised in the synthesis of both polyitaconates, which are obtained by radical polymerisation or polycondensation involving only IA, and co-polymers [6]. IA represents a valuable non-fossil derivate alternative monomer or co-monomer for the synthesis of poly(meth)acrylates due to its structural similarity to acrylic acid and methacrylic acid [7], finding application in manufacturing of resins, synthetic fibres, plastics, rubbers, surfactants, and oil additives [8–10]. Furthermore, IA functions as a building block for polymers with enhanced and innovative features, including shape memory [11], UV- and thermal-curing or crosslinking [12], biocompatibility [13, 14] and antibacterial function [15, 16]. These polymers are therefore suitable for drug delivery, tissue engineering and a wide range of biomedical applications. Recent studies have demonstrated that IA plays a crucial role in immunomodulation. IA is secreted by mammalian cells as an anti-inflammatory signal, indicating potential additional applications for this compound in the therapeutic field [17–19]. The chemical synthesis of IA was first accomplished in 1873 through the thermal decarboxylation of citric acid [20], followed by the discovery of other methods such as decarboxylation of aconitic acid and oxidation of isoprene. However, these chemical synthesis methods were not economically viable due to their low yields, low production rates, and the numerous steps involved [21, 22]. As a result, industrial production of IA relies on microbial bioprocessing using *Aspergillus terreus*, a filamentous fungus capable of producing up to 160 g/L of IA [23]. The IA biosynthetic pathway in *A. terreus* (Fig. 1) is characterized by the presence of *cis*-aconitate decarboxylase (CadA), a cytosolic enzyme that converts *cis*-aconitate into IA. Additionally,

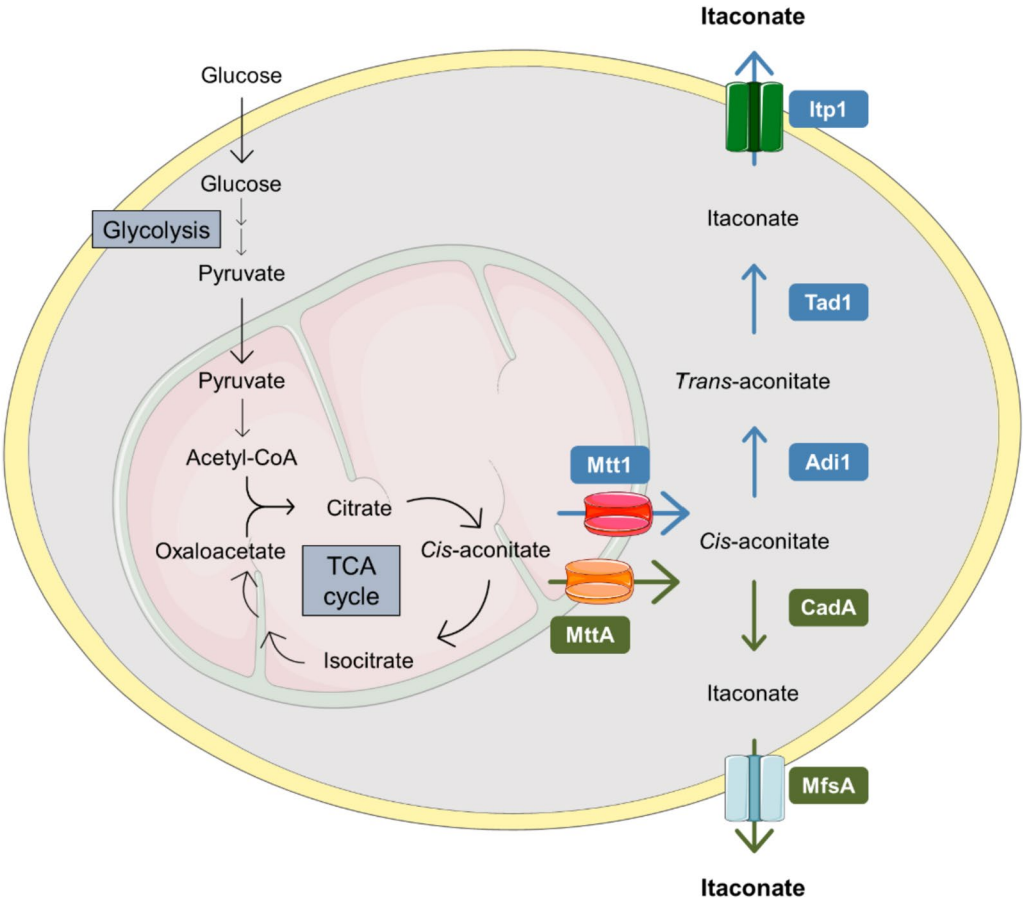

Fig. 1 Schematic representation of the IA biosynthetic and transport pathways from *A.terreus* and *U. maydis*. The figure summarizes the key enzymatic reactions and transport steps involved in the native biosynthesis of IA in both fungi. Enzymes and transporters from *A. terreus* are shown in green, while those from *U. maydis* are shown in blue. CadA, *cis*-aconitate decarboxylase (*A. terreus*); Itp1, itaconate transport protein (*U. maydis*); MttA, mitochondrial tricarboxylate transporter (*A. terreus*); Mtt1, mitochondrial tricarboxylate transporter (*U. maydis*); MfsA, major facilitator superfamily transporter (*A. terreus*); Tad1, *trans*-aconitate decarboxylase (*U. maydis*); TCA cycle, tricarboxylic acids cycle

it involves two transport proteins: the mitochondrial tricarboxylic acid transporter (MttA), which catalyses the transfer of *cis*-aconitate from the mitochondria to the cytosol, and the major facilitator superfamily transporter MfsA, which exports IA to the extracellular environment [24, 25]. However, the IA production process involving *A. terreus* as a microbial factory has several limitations. Notably, *A. terreus* is a pathogenic microorganism that can cause lethal infections, known as aspergillosis, and exhibits antibiotic resistance [26, 27]. In addition to its hazardous nature, *A. terreus* has a slow growth rate, high sugar consumption, a spore-forming life cycle, sensitivity to oxygen availability and pH of the culture medium, inhibition of IA production at low manganese ion (Mn^{2+}) concentrations (3 µg/L), mycelial shear stress associated with filamentous growth, and difficulty in genetic manipulation [28–32]. Due to these limitations, the *A. terreus* platform for IA production is difficult to manage, requiring strict control of multiple parameters.

Another natural producer of IA is *Ustilago maydis*, a unicellular yeast-like fungus pathogenic to maize crops. Unlike the *A. terreus* pathway, in *U. maydis*, IA is produced via the intermediate *trans*-aconitate (Fig. 1). The aconitase-Δ-isomerase (Adi1) converts *cis*-aconitate into *trans*-aconitate, and the *trans*-aconitate decarboxylase (Tad1) then acts on *trans*-aconitate to release IA. Both of these enzymatic activities occur in the cytosol. The pathway also includes the mitochondrial transporter (Mtt1), which facilitates the transport of *cis*-aconitate from the mitochondria to the cytosol. Finally, IA is secreted by the itaconate transporter protein Itp1 [33]. Several efficient *U. maydis* IA producing strains have been developed but this microorganism has notable drawbacks. These include its non-GRAS status, co-production of malate and succinate with IA, requiring additional separation steps, and pH sensitivity that shifts metabolism from acid production to polyol and glycolipid synthesis. These limitations necessitate

precise control of cultivation conditions, resulting in a complex production process [34–37].

To enhance IA production efficiency, genetic engineering strategies have been employed in various microorganisms, including *Aspergillus niger* [38, 39], *Saccharomyces cerevisiae* [40], *Corynebacterium glutamicum* [41], *Escherichia coli* [42–44] and *Yarrowia lipolytica* [45–48].

In this study, *Y. lipolytica* was selected as the microbial cell factory for IA production due to its numerous advantages. This non-conventional yeast is recognised as GRAS and has emerged as a promising host for heterologous IA production because of its exceptional metabolic versatility and adaptability. It benefits from advanced genetic engineering tools [49], exhibits a wide range of substrate utilisation [50], and shows tolerance to various stressors, including low pH and high substrate concentrations. These traits make it particularly suitable for the cost-effective and sustainable production of value-added bioproducts on an industrial scale. Additionally, *Y. lipolytica* exhibits a high carbon flux towards mitochondria (about 60% of the glucose carbon moles) [51]. This significant mitochondrial carbon flux results in a correspondingly high production of citrate (CA) and isocitrate (ICA), intermediates that can be efficiently utilised for IA synthesis.

The aim of this study was to efficiently produce IA using *Y. lipolytica* as a microbial platform through various genetic manipulation approaches: (1) Increasing the CA pool in the mitochondrial matrix by inactivating the gene encoding the mitochondrial citrate carrier protein, *YlYHM2*; (2) Expressing the genes from the *A. terreus* IA biosynthetic pathway (*mttA*, *cadA* and *mfsA*) in *Y. lipolytica*; (3) Eliminating the export of side metabolites, particularly CA and ICA, by deleting the membrane citrate exporter gene *YlCEX1*; (4) Introducing multiple copies of genes from the *A. terreus* pathway; (5) Evaluating the genes from the *U. maydis* IA biosynthetic pathway (*mtt1*, *adi1*, *tad1*, *itp1*), in recombinant *Y. lipolytica* strains, both alone and in combination with other genetic modifications, including the inactivation of *YlYHM2 and YlCEX1*, as well as the co-expression of the genes from the *U. maydis* and the *A. terreus* IA biosynthetic pathways. Among developed recombinant strains, the best-performing IA-producing strain of *Y. lipolytica* was identified in flask cultivation studies. This strain combined the overexpression of both the *A. terreus* and *U. maydis* IA biosynthetic pathways with the inactivation of *YlYHM2* and *YlCEX1.* The IA production process was then scaled up in a 2-L bioreactor, resulting in the most efficient IA-producing *Y. lipolytica* strain reported to date in terms of yield and productivity.

Materials and methods

Strains and culture media

Escherichia coli DH5α used for plasmid construction, propagation and amplification, was cultivated in Luria Bertani (LB) media at 37 °C with shaking (200 rpm). This medium was supplemented with antibiotics based on the resistance of the plasmids (spectinomycin (Sigma-Aldrich, St. Louis, MO, USA), 75 µg/mL; ampicillin (Sigma-Aldrich, St. Louis, MO, USA), 100 µg/mL) to allow selective growth. All *Y. lipolytica* strains constructed in this study summarised in Table 1, are derived from Y-4973, an uracil auxotroph and *Ku70*-mutant (Δ*ura3* Δ*ku70*) obtained from the W29 strain (MatA, wild-type), that shows an increased rate of homologous recombination [52].

Y. lipolytica strains were cultivated in different media at 29 °C and with orbital shaking at 200 rpm. The rich medium, used for seed culture, was YPD medium composed of 10 g/L yeast extract (Biokar Diagnostics, Allonne, France), 20 g/L peptone (Biokar Diagnostics, Allonne, France), and 20 g/L glucose (Sigma-Aldrich, St. Louis, MO, USA). Whenever required, the medium was supplemented with nourseothricin (Jena Bioscience, Jena, Germany) (350 µg/mL) for the overnight growth of *Y. lipolytica* strains transformed with Cas9 expressing plasmids, or with hygromycin (Sigma-Aldrich, St. Louis, MO, USA) (450 µg/mL) for selective marker recovery procedure. The minimal medium was composed of 1.7 g/L Yeast Nitrogen Base without nitrogen source (YNB) (Difco™, Becton Dickinson, Sparks, MD, USA) supplemented with glucose and ammonium sulphate (VWR Chemicals, Radnor, PA, USA) at various concentrations based on the scope of the cultivation, achieving different Carbon to Nitrogen (C/N) ratio.

For uracil auxotrophic strains, the minimal medium was supplemented with 0.3 g/L uracil (Sigma-Aldrich, St. Louis, MO, USA). For selection of *URA3* marker-based transformants, the minimal medium was supplemented with 20 g/L glucose, 5 g/L ammonium sulphate, and 2 g/L of each of the 20 proteinogenic amino acids (Sigma-Aldrich, St. Louis, MO, USA), without uracil. Solid media were prepared by adding 20 g/L of bacteriological agar (Type E, Biokar Diagnostics, Allonne, France).

Construction of plasmids and recombinant strains

Plasmids for yeast genome engineering were constructed using a set of vectors from the synthetic biology toolkit *YaliCraft* as backbones [52]. For the transformation of *Y. lipolytica* strains, both a Cas9-helper plasmid (encoding Cas9 and a guide RNA, or gRNA), and a repair fragment with homologous flanking regions for genome integration (Donor) were used. After the endonuclease

Table 1 *Y. lipolytica* strains used in this study and their genotype. Genotypes are presented in the format [integration site]:[promoter]-[gene]-[terminator], where the integration site (Int) refers to the specific genomic locus targeted, as described by Yuzbashev et al. (2023). The promoter (p) and terminator (t) elements vary depending on the expression cassette used. The overexpressed gene is shown in italics

Strain	Genotype	Reference
Y-4972	W29 Δ*ku70*	Yuzbashev et al., 2023
Y-4973	W29 Δ*ku70* Δ*ura3*	Yuzbashev et al., 2023
YM4B222	Y-4973 Δ*Ylyhm2*	This study
YM4B246	YM4B222 Δ*Ylcex1*	This study
YM4B256	YM4B222 IntC2:pTEF1-*cadA*-tLIP2/pGADPH-*mttA*-tScPGK1/pFBA1-*mfsA*-tScADH1	This study
YM4B324	YM4B256 Δ*Ylcex1*	This study
YM4B364	YM4B324 IntE16:pEXP1-*cadA*-tScADH1	This study
YM4B371	YM4B324 IntF9:pFBA1-*mfsA*-tScADH1	This study
YM4B372	YM4B324 IntE8-pGADPH-*mttA*-tScPGK1	This study
YM4B373	YM4B364 IntF9:pFBA1-*mfsA*-tScADH1	This study
YM4B374	YM4B324 IntE15:pTEF1-*cadA*-tLIP2/pGADPH-*mttA*-tScPGK1/pFBA1-*mfsA*-tScADH1	This study
YM4B461	Y-4973 IntC2:pTEF1-*cadA*-tLIP2/pGADPH-*mttA*-tScPGK1/pFBA1-*mfsA*-tScADH1	This study
YM4B491	Y-4973 IntF11:pTEF1-*adi1*-tScPGK1/pEXP1-*tad1*-tScENO2 IntB11:pTEF1-*mtt1*-tScADH1/pEXP1-*itp1*-tLIP2	This study
YM4B492	YM4B246 IntF11:pTEF1-*adi1*-tScPGK1/pEXP1-*tad1*-tScENO2 IntB11:pTEF1-*mtt1*-tScADH1/pEXP1-*itp1*-tLIP2	This study
YM4B493	YM4B324 IntF11:pTEF1-*adi1*-tScPGK1/pEXP1-*tad1*-tScENO2 IntB11:pTEF1-*mtt1*-tScADH1/pEXP1-*itp1*-tLIP2	This study

Cas9 created a double-strand break at a specific genomic locus, directed by the gRNA (a 20 nt RNA sequence), the Donor was integrated into the genome via the homologous recombination (HR) repair mechanism. The integration loci, identified as intergenic regions, have been previously described [52]. For the *YlYHM2* gene (YALI1_B14382g) inactivation, the deletion cassette Δ*Ylyhm2* was produced via PCR amplification of a genomic fragment from the previously described Δ*Ylyhm2* strain [53]. To inactivate the *YlCEX1* gene (YALI1_E32636g), a deletion cassette (Δ*Ylcex1*) was created by PCR amplification of the 803 bp upstream and 820 bp downstream regions of the coding DNA sequence (CDS) from the wild-type strain Y-4973, using specific primers listed in Table S1. These two fragments were then combined using overlapping extension PCR to form the deletion cassette. Transformations were performed using the deletion cassettes along with the pCasNA-RK helper plasmid expressing Cas9. This plasmid also included sequences encoding specific gRNAs for *YlYHM2* or *YlCEX1* (Table S1). The gRNAs were designed using the ChopChop tool (http://chopchop.cbu.uib.no/) and inserted as previously described [52]. The deletions were verified by PCR amplification on the genome of transformant strains using primers flanking the *YlYHM2* or *YlCEX1* genes, respectively (Table S1).

To overexpress the IA biosynthetic genes from *A. terreus* (*cadA*, *mttA*, *mfsA*) and *U. maydis* (*adi1*, *itp1*, *mtt1*, *tad1*), plasmids were constructed using the Golden Gate assembly method [54]. This involved using BsaI as the restriction enzyme and combining plasmid components from the *YaliCraft* toolkit, particularly from the Exp Module. A single transcriptional unit was assembled using an empty Level 1 plasmid, which determined the integration locus of the final construct. The selected empty Level 1 vector was combined with two Level 0 plasmids, each containing a promoter (from the pPro series) and a terminator (from the pTer series), along with the CDS as synthetic *Y. lipolytica*-codon-optimised DNA including specific overhangs with corresponding restriction sites compatible with Golden Gate assembly (Table S2). Then, up to three transcriptional units were combined in Level 2 plasmids through the utilisation of the Golden Gate assembly method using BsmBI as the restriction enzyme. In this one-pot reaction, a selected empty Level 2.2 or 2.3 vector was combined with two (Level 1.1 and 1.2) or three (Level 1.1, 1.2 and 1.3) assembled Level 1 plasmids. The expression cassettes were released from the plasmids by digestion with the NotI endonuclease, resulting in donor DNA used in the CRISPR/Cas9-based genome engineering of *Y. lipolytica*. To integrate the overexpression constructs into yeast strains, the corresponding donor was co-transformed with the Cas9-helper, targeting a specific locus in the *Y. lipolytica* genome. The *URA3* gene served as the selection marker for the overexpression constructs, making the transformed strains prototrophic for uracil. For each subsequent step, an auxotrophic derivative was obtained using the Cre-lox 66/71 recombination system, as previously described [52, 55]. To verify the correct

chromosomal integration, PCR was performed using primers annealing to the flanking regions of the integration locus (Table S1). The complete set of plasmids used in this study is reported in Table S3.

Shake flask cultures

The recombinant strains were tested in cultivation studies to verify the effect of the genetic modification on the product profile. Growth curves and the production of organic acids by *Y. lipolytica* strains were monitored in YNB medium supplemented with 90 g/L glucose and 2 g/L ammonium sulphate (C/N ratio of 85). Cultivation was carried out in 250-mL baffled flasks containing 50 mL of medium for 10 days in an orbital shaker at 29 °C and 200 rpm. The medium's pH was buffered by adding sterile 10 g/L $CaCO_3$ (Sigma-Aldrich, St. Louis, MO, USA) after 4–6 h of incubation. Cells were inoculated from an overnight seed culture in YPD to an initial optical density (OD_{600}) of 0.1.

Bioreactor fermentation process

Fed-Batch fermentation was conducted in a 2.0 L bioreactor (BIOSTAT B Plus; Sartorius, Germany) with a starting working volume of 0.7 L. The bioreactor production medium consisted of YNB (1.7 g/L) supplemented with either glucose or glycerol (Sigma-Aldrich, St. Louis, MO, USA) (each at 30 g/L) and ammonium sulphate (3 g/L). The seed culture was grown for 24 h in a 250-mL baffled flask containing 50 mL of YPD medium. The bioreactor was inoculated at an initial OD_{600} 1.0 and the cultivation was conducted for a period of 9 days. The agitation rate was maintained at 800 rpm, while the aeration rate was initially set at 1.0 vvm for the first 48 h and then reduced to 0.7 vvm. The pH was automatically maintained at 6.0 by adding a 40% NaOH solution. Approximately every 24 h, the culture was fed with the carbon source (glucose or glycerol) and ammonium sulphate. Glucose or glycerol were added based on the measured consumption from the previous 24 h, with a 10% increase. Accordingly, ammonium sulphate was added to maintain a C/N ratio of 94. A silicone-based anti-foaming emulsion 30 (Carl Roth GmbH, Germany) was used.

Analytical methods

The flask cultivations were monitored by measuring the growth of the yeast cells using a spectrophotometer to determine OD_{600}. The supernatant was collected after neutralising $CaCO_3$ with a 1 M HCl solution and separating the cells by centrifugation at 12,000 g for 5 min. The supernatant was then stored at −20 °C until analysis. The bioreactor cultivation was monitored by sampling 10 mL every 24 h. The supernatant was analysed by HPLC using an Alliance 2695 separation module (Waters, Milford, MA, USA) coupled with a Waters 2996 UV detector and a Waters 2410 refractive index detector. For organic acid detection, a Kinetex EVO C18 column (150 mm ×4.6 mm, 100 Å, 5 µm) (Phenomenex Inc., USA) was used with 0.010 M H_3PO_4 at pH 1.5 as the mobile phase, coupled to a UV detector set at 220 nm. For glucose and glycerol measurement, a Rezex ROA-Organic Acid H+ (8%) column (300 mm ×7.8 mm) (Phenomenex Inc., USA) was used with 0.0025 M H_2SO_4 as the mobile phase and a refractive index detector set at 410 nm. Samples were quantified by comparison with commercial standards. Dry cell weight (DCW) was estimated after harvesting the biomass by centrifugation at 12,000 g for 5 min, prefreezing at −20 °C, and freeze-drying using a Labconco FreeZone 2.5 Liter Benchtop Freeze Dryer operating at −50 °C and 0.05 mbar for 48 h.

Results

Enhancing the mitochondrial CA pool

IA is synthesised through the cytosolic decarboxylation of *cis*-aconitate, which is in turn produced in mitochondria from CA. Therefore, the initial step in the metabolic engineering strategy was to increase the mitochondrial pool of CA. This was accomplished by deleting the *YlYHM2* gene. During growth on glucose, YlYhm2 is the main mitochondrial citrate transporter in *Y. lipolytica* [53]. The obtained strain YM4B222 (W29 Δ*ku70* Δ*ura3* Δ*Ylyhm2*) secreted solely ICA with a final titre of 10.23 ± 0.97 g/L after 240 h (Fig. 2A), achieving a yield of 0.107 ± 0.010 mol/mol ($Y_{ICA/GLU}$) (Fig. 2B). For comparison, the wild-type-derived strain Y-4973 (W29 Δ*ura3* Δ*ku70*) produced 13.85 ± 2.81 g/L CA and 2.21 ± 0.65 g/L ICA after 240 h of cultivation (Fig. 2A). The highest titres were observed at 120 h of cultivation, reaching 26.94 ± 2.25 g/L CA and 4.36 ± 0.35 g/L ICA (Figure S1). The deletion of *YlYHM2* gene resulted in a significant increase in ICA secretion ($P < 0.001$) compared to the wild-type strain; however, it also showed a 22% decrease of biomass accumulation after 240 h of cultivation (Fig. 2A).

Establishing the *A. terreus* IA biosynthetic pathway in *Y. lipolytica*

To produce IA, the *A. terreus* pathway was introduced by overexpressing its three key genes (*cadA*, *mttA*, and *mfsA*) in two *Y. lipolytica* strains (Figure S2): the wild-type strain Y-4973 (W29 Δ*ku70* Δ*ura3*) and the recombinant strain YM4B222 (W29 Δ*ku70* Δura3 Δ*Ylyhm2*), described in the previous section.

Table S3 presents the detailed description of the transcriptional units used in the genetic manipulations. The recombinant strains YM4B461 (W29 Δ*ku70* IntC2:*cadA-mttA-mfsA*) and YM4B256 (W29 Δ*ku70* Δ*Ylyhm2* IntC2:*cadA-mttA-mfsA*) were tested in flask cultivations

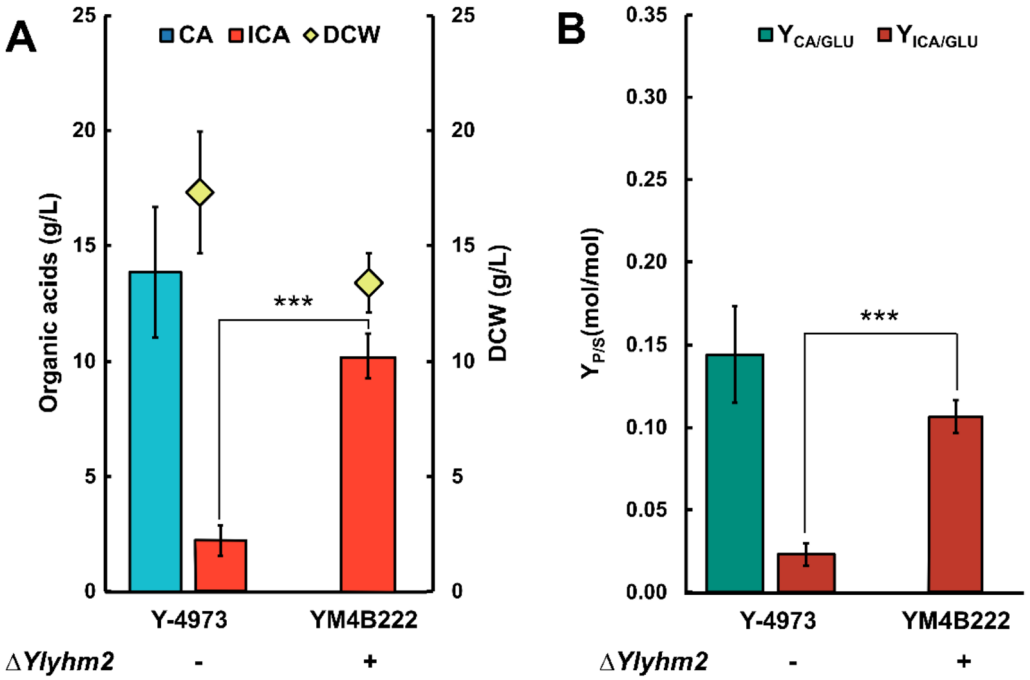

Fig. 2 Effect of *YlYHM2* gene deletion on organic acids synthesis. *Y. lipolytica* strains were cultivated in 250-mL baffled flasks for 10 days. (**A**) Organic acids and biomass titre (Dry Cell Weight) and (**B**) yields of organic acids on glucose for wild-type strain Y-4973 and recombinant strain YM4B222. CA, citric acid; DCW, Dry Cell Weight; GLU, glucose; ICA, isocitric acid; $Y_{P/S}$, yield of product on substrate. Data represent the mean of at least three independent experiments and error bars represent standard error. The statistical significance was determined using an unpaired Student's *t*-test (*** $P < 0.001$)

(Figure S3) using minimal medium supplemented with excess of glucose and nitrogen restriction. After 240 h of cultivation, strain YM4B461, derived from the wild-type background (Figure S2), exhibited a low but detectable level of IA production (1.51 ± 0.01 g/L), with a final biomass concentration of 18.05 ± 3.08 g/L (Fig. 3A). The final yield of IA was 0.023 ± 0.002 mol/mol ($Y_{IA/GLU}$) (Fig. 3B). Additionally, CA and ICA were detected in the medium, reaching a final concentration of 12.01 ± 0.29 g/L and 5.83 ± 0.10 g/L, respectively (Fig. 3A). These values correspond to final yields on glucose of 0.125 ± 0.002 mol/mol ($Y_{CA/GLU}$) for CA and 0.061 ± 0.001 mol/mol ($Y_{ICA/GLU}$) for ICA (Fig. 3B). The CA/ICA ratio was 2.1, compared to 6.3 observed during the cultivation of the wild-type strain. Consequently, the introduction of the IA biosynthetic pathway not only facilitated IA accumulation but also significantly increased ICA production, reaching levels 2.7-fold higher than those observed in the wild-type Y-4973.

In strain YM4B256, which features the *A. terreus* IA biosynthetic pathway genes and the *YlYHM2* deletion (Figure S2), the final IA titre reached 2.88 ± 0.38 g/L (Fig. 3A) with a yield on glucose of 0.040 ± 0.005 mol/mol ($Y_{IA/GLU}$) (Fig. 3B) under the same cultivation conditions. As a result, the deletion of the *YlYHM2* gene led to a statistically significant 1.9-fold increase in IA production ($P < 0.05$) compared to the strain with only the IA biosynthetic pathway, while achieving a similar biomass level (20.31 ± 2.99 g/L) (Fig. 3A). Surprisingly, in the strain YM4B256, in addition to ICA, CA secretion was restored with a final titre of 8.44 ± 0.93 g/L (Fig. 3A), possibly due to the activity of a cytosolic aconitase. At 240 h, CA and ICA showed a final yield of 0.092 ± 0.010 mol/mol ($Y_{CA/GLU}$) and 0.070 ± 0.008 mol/mol ($Y_{ICA/GLU}$), respectively (Fig. 3B).

Enhancing IA production level and selectivity through *YlCEX1* gene deletion

To further enhance IA production and minimise by-product secretion (i.e., CA and ICA), the *YlCEX1* gene, which encodes the plasma membrane citrate exporter, was deleted in strain YM4B256. Previous studies demonstrated that inactivating *YlCEX1* completely eliminated CA and ICA secretion into the cultivation medium [56]. The resulting strain YM4B324 (W29 Δ*ku70* Δ*Ylyhm2* IntC2:*cadA-mttA-mfsA* Δ*Ylcex1*) (Figure S4), exhibited a higher IA production while maintaining a comparable final biomass titre (16.70 ± 2.28 g/L) (Fig. 4A). After 240 h of cultivation, IA reached a concentration of 8.03 ± 0.53 g/L (Fig. 4A), representing a 2.8-fold increase compared

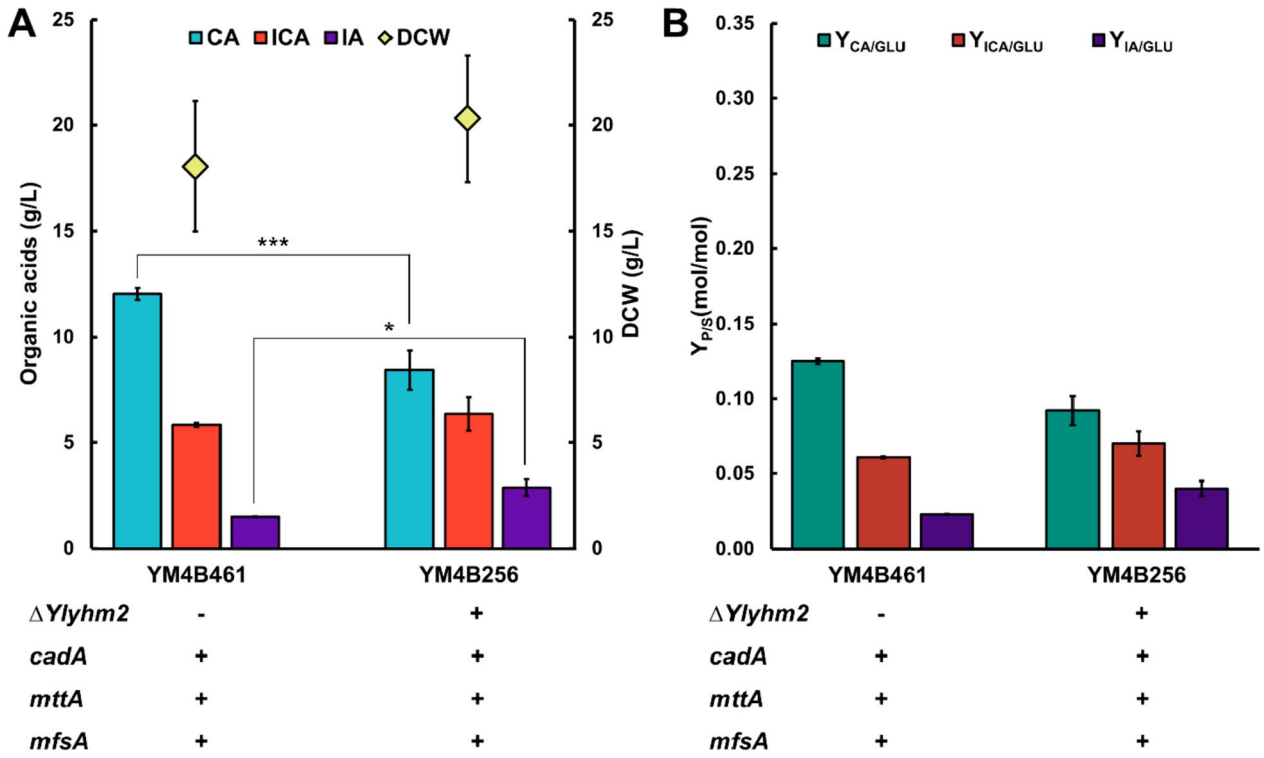

Fig. 3 Establishing the *A. terreus* IA biosynthetic pathway in *Y.lipolytica*. *Y. lipolytica* strains were cultivated in 250-mL baffled flasks for 10 days. (**A**) Organic acids and biomass titre (Dry Cell Weight) and (**B**) yields of organic acids on glucose for recombinant strains YM4B461 and YM4B256. CA, citric acid; DCW, Dry Cell Weight; GLU, glucose; ICA, isocitric acid; IA, itaconic acid; $Y_{P/S}$, yield of product on substrate. Data represent the mean of at least three independent experiments, with error bars indicating the standard error. The statistical significance was determined using an unpaired Student's t-test (* $P < 0.05$, *** $P < 0.001$)

to the parental strain YM4B256. Moreover, no CA, ICA, or other organic acids were detected in the cultivation medium (Figure S6), indicating that *YlCEX1* deletion effectively shifted the balance CA-IA transformation towards the latter. Despite the enhanced IA production, the yield on the substrate remained relatively low (0.124 ± 0.008 mol/mol $Y_{IA/GLU}$) (Fig. 4B).

Optimizing IA production through multi-gene insertion strategy

To further increase IA production, multiple copies of *A. terreus* biosynthetic pathway genes were integrated in *Y. lipolytica* strains (Figure S5). For this purpose, single transcription units containing individual genes from the biosynthetic pathway were used (Table S3). The recombinant strains were tested in flask cultivation for 10 days incubated at 29 °C and 200 rpm, using minimal medium supplemented with excess of glucose and nitrogen restriction (Figure S6).

A transcriptional unit with the *cadA* gene was integrated into an additional genomic locus of the best-performing strain from the previous step, YM4B324. The resulting strain, YM4B364 (W29 Δ*ku70* Δ*Ylyhm2* IntC2:*cadA-mttA-mfsA* Δ*Ylcex1* IntE16:*cadA*) (Figure S5), achieved a final IA titre of 9.50 ± 1.07 g/L (Fig. 4A), corresponding to an 18% increase in IA yield (0.146 ± 0.015 mol/mol $Y_{IA/GLU}$) compared to the parental strain YM4B324, which carried a single copy of the *cadA* gene (Fig. 4B). This result is consistent with a previous study reporting that multiple copies of *cadA* enhanced IA production [46]. Alternatively, a second copy of the *mfsA* gene, encoding a major facilitator superfamily transporter, was introduced into strain YM4B324. However, this modification did not lead to increased IA production. The resulting strain, YM4B371 (W29 Δ*ku70* Δ*Ylyhm2* IntC2:*cadA-mttA-mfsA* Δ*Ylcex1* IntF9:*mfsA*) (Figure S5), accumulated 7.37 ± 0.39 g/L of IA (Fig. 4A) with a yield of 0.113 ± 0.006 mol/mol ($Y_{IA/GLU}$) (Fig. 4B). Similarly, a strain carrying additional copies of both *cadA* and *mfsA*, designated as YM4B373 (W29 Δ*ku70* Δ*Ylyhm2* IntC2:*cadA-mttA-mfsA* Δ*Ylcex1* IntE16:*cadA* IntF9:*mfsA*) (Figure S5), exhibited a decrease in IA production, yielding 6.76 ± 1.25 g/L (Fig. 4A). The reduced production of IA in the two recombinant strains, YM4B371 and YM4B373, which carry a second copy of the *mfsA* gene, is probably due to the metabolic burden

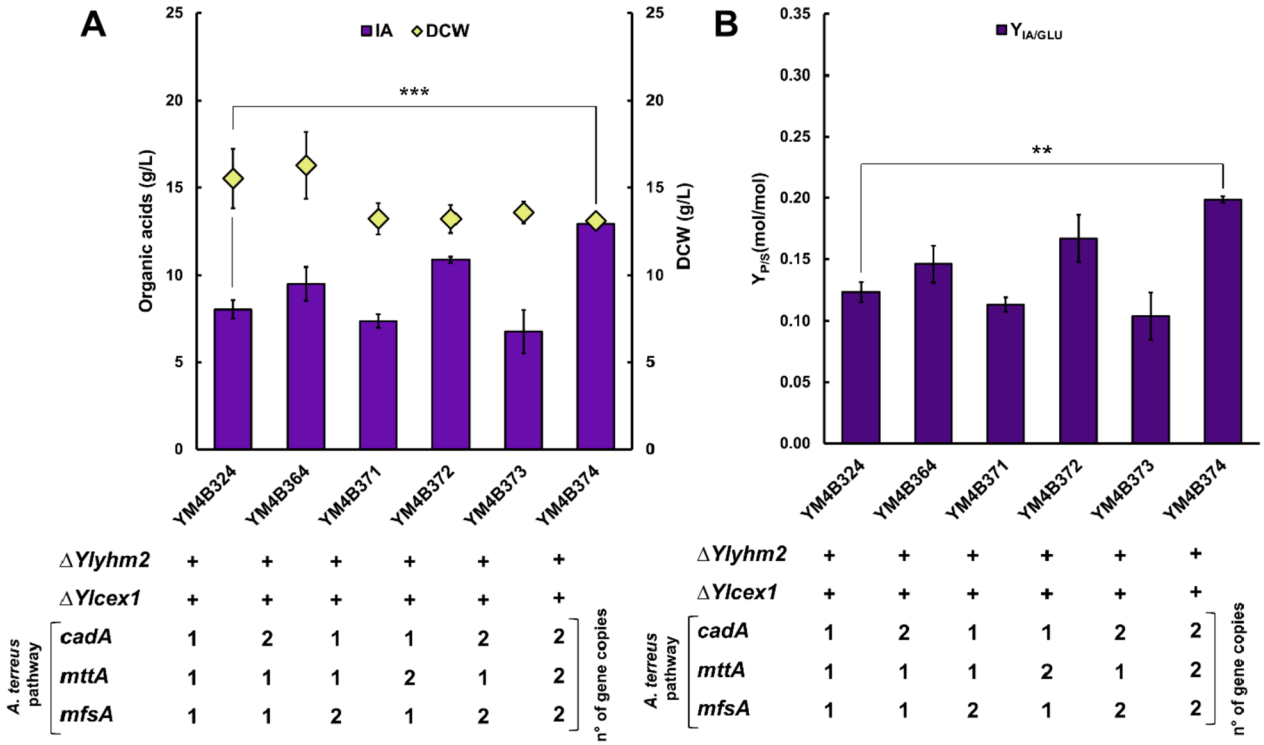

Fig. 4 Effect of *YlCEX1* deletion and multi-gene insertion strategy on IA production. *Y. lipolytica* strains were cultivated in 250-mL baffled flasks for 10 days. (**A**) Organic acids and biomass titre (Dry Cell Weight) and (**B**) yields of organic acids on glucose for recombinant strains YM4B324, YM4B364, YM4B371, YM4B372, YM4B373 and YM4B374. DCW, Dry Cell Weight; GLU, glucose; IA, itaconic acid; $Y_{P/S}$, yield of product on substrate. Data represent the mean of at least three independent experiments, with error bars indicating the standard error. The statistical significance of IA production was assessed using one-way ANOVA followed by Dunnett's multiple comparisons test, with strain YM4B324 serving as the reference (** $P < 0.01$, *** $P < 0.001$).

imposed on cells overexpressing a plasma membrane protein.

In addition, a second copy of the *mttA* gene, encoding for the mitochondrial *cis*-aconitate transporter, was introduced into strain YM4B324. This modification led to an improvement in IA production. The resulting strain, YM4B372 (W29 *Δku70 ΔYlyhm2* IntC2:*cadA-mttA-mfsA ΔYlcex1* IntE8:*mttA*) (Figure S5), achieved an IA titre of 10.84 ± 0.18 g/L (Fig. 4A), representing a 35% increase compared to YM4B324, with a yield of 0.167 ± 0.019 mol/mol ($Y_{IA/GLU}$) (Fig. 4B).

Finally, a recombinant strain carrying two complete copies of the IA biosynthetic pathway from *A. terreus*, integrated in two different genomic loci (C2 and E15), was constructed. This strain, YM4B374 (W29 *Δku70 ΔYlyhm2* IntC2:*cadA-mttA-mfsA ΔYlcex1* IntE15:*cadA-mttA-mfsA*) (Figure S5), produced a IA final titre of 12.91 ± 0.17 g/L (Fig. 4A), corresponding to a statistically significant 61% increase compared to parental strain YM4B324 ($P < 0.01$). The IA yield on glucose was the highest among the recombinant strains with multiple copies of IA biosynthetic pathway from *A. terreus*, reaching 0.199 ± 0.003 mol/mol ($Y_{IA/GLU}$) (Fig. 4B).

Biomass formation in strains overexpressing multiple copies of the genes of the IA biosynthetic pathway from *A. terreus* was slightly lower compared to the parental strain YM4B324, which carried a single copy of these genes. An exception was strain YM4B364, which carried an additional copy of the *cadA* gene and exhibited a 5% increase in biomass compared to YM4B324. Conversely, the other recombinant strains showed approximately 15% lower biomass concentrations than the parental strain (Fig. 4A). However, an inverse correlation between IA production and biomass accumulation was not observed.

Evaluation of *U. maydis* IA biosynthetic pathway in *Y. lipolytica*

The production of IA through *trans*-aconitate was subsequently evaluated by introducing an alternative pathway derived from *U. maydis* (Figure S7). To assess the *U. maydis* IA biosynthetic pathway, four corresponding genes (*adi1*, *tad1*, *mtt1*, and *itp1*) were overexpressed in two

different genomic loci. Three different parental strains were tested as recipients: the wild-type strain (Y-4973), a strain with inactivated *YlYHM2* and *YlCEX1* genes (YM4B246), and the strain with inactivated *YlYHM2* and *YlCEX1* along with the overexpression of the *A. terreus* IA biosynthetic pathway (YM4B324). These strains were tested in flask cultivation for 10 days incubated at 29 °C and 200 rpm, using minimal medium supplemented with excess of glucose and nitrogen restriction (Figure S8).

In strain YM4B491 (W29 Δ*ku70* IntF11:*adi1-tad1* IntB11:*mtt1-itp1*) (Figure S7), overexpression of the *U. maydis* pathway alone resulted in the accumulation of only trace amounts of IA (0.09 ± 0.03 g/L) (Fig. 5B). Instead, a considerable accumulation into the extracellular phase of CA and ICA was observed, with a final production of 13.03 ± 1.46 g/L and 2.31 ± 0.26 g/L, respectively (Fig. 5B), corresponding to a yields of 0.140 ± 0.010 mol/mol ($Y_{CA/GLU}$) and 0.024 ± 0.009 mol/mol ($Y_{ICA/GLU}$), respectively (Fig. 5C). Biomass formation was 13.55 ± 1.07 g/L, with a 25% decrease compared to the corresponding strain YM4B461 carrying the genes of the *A. terreus* IA biosynthetic pathway.

In contrast, strain YM4B492 (W29 Δ*ku70* Δ*Ylyhm2* Δ*Ylcex1* IntF11:*adi1-tad1* IntB11:*mtt1-itp1*) (Figure S7) in which the genes of the *U. maydis* pathway were overexpressed together with the deletions of *YlYHM2* and *YlCEX1*, accumulated 0.49 ± 0.01 g/L of IA (Fig. 5B). Similar to YM4B324 strain (expressing the genes of the *A. terreus* IA pathway in the Δ*Ylyhm2* Δ*Ylcex1* background), no CA or ICA secretion was observed, and biomass formation reached 16.96 ± 1.98 g/L (Fig. 5B), resulting in a 16% decrease compared to the corresponding strain YM4B324. Thus, the overexpression of the genes of the *U. maydis* pathway in strains with these two different genetic backgrounds did not lead to IA production comparable to those achieved by strains overexpressing the genes of the *A. terreus* pathway.

However, when both IA biosynthetic pathways, from *A. terreus* and *U. maydis*, were combined in single strain with deletions of both *YlYHM2* and *YlCEX1*, the resulting strain YM4B493 (W29 Δ*ku70* Δ*Ylyhm2* Δ*Ylcex1* IntC2:*cadA-mttA-mfsA* IntF11:*adi1-tad1* IntB11:*mtt1-itp1*) (Fig. 5A) accumulated IA at final titre of 19.66 ± 0.36 g/L after 240 h of cultivation (Fig. 5B), with a yield of 0.303 ± 0.006 mol/mol ($Y_{IA/GLU}$) (Fig. 5C). This represented a 2.5-fold increase in IA production compared to the parental strain YM4B324, which carried only the genes of the *A. terreus* pathway. Biomass formation reached a final titre of 11.27 ± 0.28 g/L (Fig. 5B), which corresponded to the lowest concentration observed among all the recombinant strains. These findings suggests that extensive strain engineering may have a slight toxic effect on yeast growth. Both strains (YM4B374 and YM4B493) expressing two copies of the genes of the IA biosynthetic pathways (either 2 copies of the genes of the *A. terreus* pathway or 1 copy of the genes of the *A. terreus* + 1 copy of the genes of the *U. maydis* pathways) showed the lowest biomass accumulation levels (13.08 and 11.27 g/L respectively).

Fed-batch cultivation of the best IA producing strain

Bioreactor cultivations of the highest-performing IA producer strain YM4B493 (W29 Δ*ku70* Δ*Ylyhm2* Δ*Ylcex1* IntC2:*cadA-mttA-mfsA* IntF11:*adi1-tad1* IntB11:*mtt1-itp1*) were carried out under controlled conditions using pulse-feeding of either glucose or glycerol as carbon sources (Fig. 6). Concurrently, nitrogen was supplemented to adjust the C/N ratio to 94, thereby inducing nitrogen limitation, a condition known to enhance organic acid production [57]. The average substrate consumption rates were comparable between the two carbon sources, resulting in 1.01 g/L/h for glucose and 0.90 g/L/h for glycerol. The highest IA titres were achieved at the end of the fermentation (215 h), reaching 55.08 g/L with glucose and 37.71 g/L with glycerol, respectively.

The IA yield was 0.343 mol/mol ($Y_{IA/GLU}$) when glucose was used as the carbon source and 0.134 mol/mol ($Y_{IA/GLY}$) with glycerol, respectively. The lower yield observed with glycerol could be attributed to the formation of side-metabolites, including *cis*-aconitate, malate,

(See figure on next page.)

Fig. 5 Evaluation of *U. maydis* IA biosynthetic pathway in *Y. lipolytica*. *Y. lipolytica* strains were cultivated in 250-mL baffled flasks for 10 days. (**A**) Schematic representation of the genetic modifications in strain YM4B493, including the inactivation of *YlYHM2* and *YlCEX1* genes (shown in red boxes) and the overexpression of heterologous genes from the IA pathway of *A. terreus* (*cadA*, *mttA*, *mfsA*) and *U. maydis* (*mtt1*, *adi1*, *tad1*, *itp1*) (shown in green boxes). (**B**) Organic acids and biomass titre (Dry Cell Weight) and (**C**) yields of organic acids on glucose for recombinant strains YM4B491, YM4B492 and YM4B493. *CEX1*, plasma membrane citrate/isocitrate exporter; DCW, Dry Cell Weight; GLU, glucose; IA, itaconic acid; *itp1*, itaconate transport protein (*U. maydis*); *mttA*, mitochondrial tricarboxylate transporter (*A. terreus*); *mtt1*, mitochondrial tricarboxylate transporter (*U. maydis*); *mfsA,* major facilitator superfamily transporter (*A. terreus*); *tad1*, *trans*-aconitate decarboxylase (*U. maydis*); TCA cycle, tricarboxylic acids cycle; *YHM2*, mitochondrial citrate-α-ketoglutarate carrier. Data represent the mean of at least three independent experiments, with error bars indicating the standard error. The statistical significance of IA production was determined using an unpaired Student's *t*-test (** $P < 0.01$, *** $P < 0.001$). **a**, **b** indicate a statistically significant difference ($P < 0.05$) in biomass production (g DCW/L) for strain YM4B493 compared to YM4B491 and YM4B492 strains

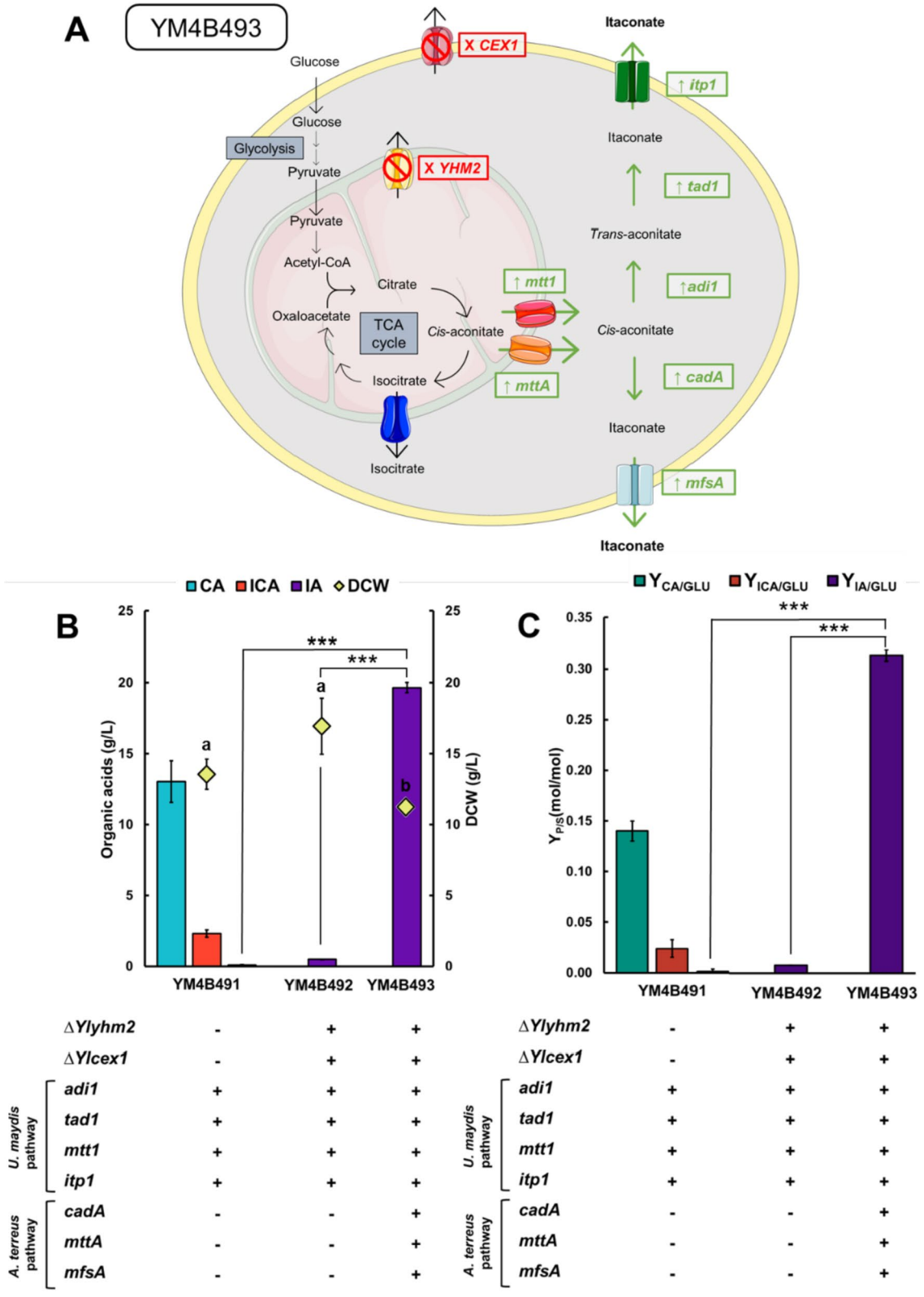

Fig. 5 (See legend on previous page.)

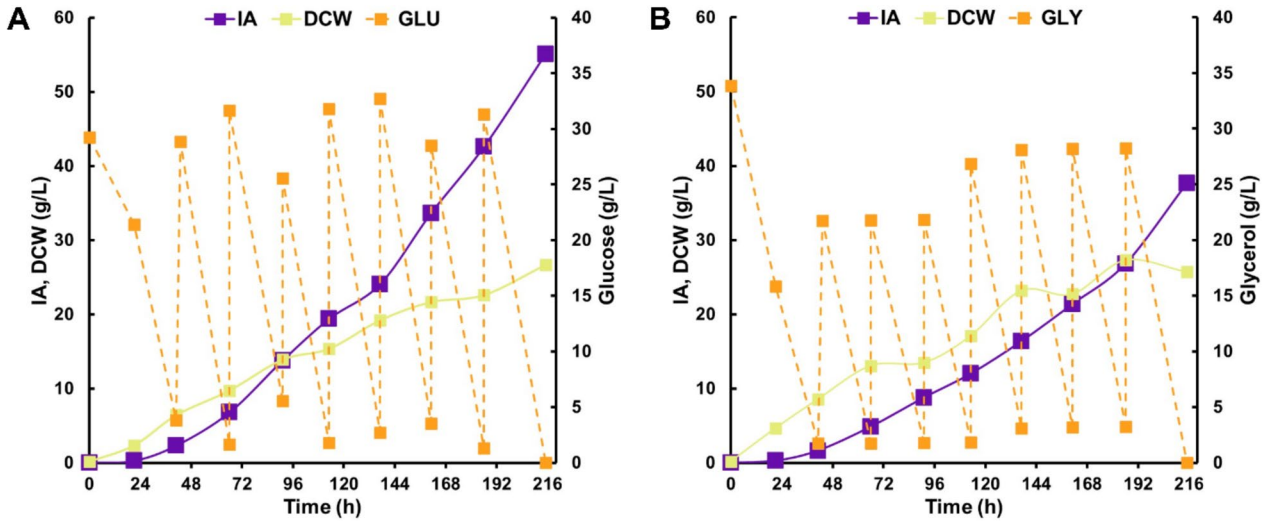

Fig. 6 IA production by strain YM4B493 during fed-batch cultivations in bioreactor. Cultivation on (**A**) glucose and (**B**) glycerol of the recombinant strain YM4B493 (W29 Δ*ku70* Δ*Ylyhm2* Δ*Ylcex1* IntC2:*cadA-mttA-mfsA* IntF11:*adi1-tad1* IntB11:*mtt1-itp1*) for 9 days. DCW, Dry Cell Weight; GLU, glucose; GLY, glycerol; IA, itaconic acid. The data depict an individual representative experiment

mannitol, pyruvate, and succinate, which were quantitatively detected in the fermentation broth at an average concentration of approximately 1 g/L (data not shown). In contrast, glucose-fed cultivation exhibited succinate as the sole detectable by-product, with a final concentration of 3.42 g/L. The highest IA productivity was recorded during the late stages of cultivation, between 137 and 215 h, reaching a rate of 1.67 g/L/h with glucose and 1.08 g/L/h with glycerol. The overall average IA productivities across the entire cultivation period were 0.256 g/L/h for glucose and 0.175 g/L/h for glycerol.

Discussion

The aim of this study was to develop a microbial platform for IA production, a building block with applications in several industrial sectors, particularly polymer synthesis. Using various metabolic engineering strategies, a recombinant *Y. lipolytica* strain capable of producing high levels of IA, without significant levels of other by-products, was successfully obtained. Two different biosynthetic pathways for the production of IA in the *Y. lipolytica* strain were evaluated. IA is naturally produced at high titres by two fungi, *A. terreus* and *U. maydis* [24, 25]. In this study, plasmids carrying the complete set of genes involved in the IA biosynthetic pathway from *A. terreus* (*cis*-pathway) and *U. maydis* (*trans*-pathway) were successfully assembled, introduced into *Y. lipolytica* strains with the same genetic backgrounds, and compared.

The genes of the *A. terreus cis*-pathway were found to be significantly more effective than the genes of the *U. maydis trans*-pathway. Several factors may account for this difference, including the one-step conversion catalysed by CadA in the *cis*-pathway in contrast to the two-step conversion mediated by Adi1 and Tad1 in the *trans*-pathway. Furthermore, CadA exhibits a higher catalytic rate constant and a lower Michaelis constant for *cis*-aconitate, compared to the combined activities of Adi1 and Tad1 [33, 58, 59]. Differences in transport mechanisms between MttA and Mtt1, particularly in terms of kinetics and counter-substrate specificity, may also contribute to the observed differences [60]. The findings of this study are in contrast with previous report. Fu *et al.* (2024) reported that the sole overexpression of *adi1* and *tad1* in *Y. lipolytica* resulted in IA production levels 155% higher than those achieved by the sole overexpression of *cadA* gene. This finding suggests that the enzymatic activities of Adi1 and Tad1 from *U. maydis* are more efficient in converting *cis*-aconitate to IA than the CadA from *A. terreus*. However, when *adi1* and *tad1* were co-expressed with *mttA* from *A. terreus*, IA production was lower than in strains overexpressing both *cadA* and *mttA*, indicating that the catalytic efficiency of *U. maydis* enzymes diminishes when combined with the mitochondrial tricarboxylate transporter from *A. terreus* [46].

The strain expressing only the *A. terreus cis*-pathway showed low IA production and poor selectivity due to co-secretion of CA and ICA. To improve this, metabolite fluxes were redirected by manipulating key transport proteins. Inactivation of the mitochondrial citrate carrier (*YlYHM2*) and the membrane citrate exporter (*YlCEX1*) significantly reduced CA and ICA levels. This strategy also aimed to increase the mitochondrial CA

and *cis*-aconitate pools, thereby enhancing IA synthesis in the cytosol.

The results showed that combining the overexpression of the genes from the *A. terreus* pathway with the inactivation of the *YlYHM2* gene resulted in a 1.9-fold increase in IA titre compared to the strain overexpressing only the *cis*-pathway. It is important to note that the *YlYHM2* deletion results in the absence of CA secretion. However, introducing the *A. terreus* IA biosynthetic pathway into this strain restores CA secretion. To explain the recovery of CA production in the strain lacking the *YlYHM2* gene and overexpressing the IA biosynthetic pathway genes, it can be hypothesised that increased levels of *cis*-aconitate may promote its conversion to CA through a cytosolic aconitase activity. As reported in *S. cerevisiae* [61], *Y. lipolytica* aconitase may also have a dual localisation, being present in both the mitochondria and the cytosol. The accumulation of cytosolic *cis*-aconitate is likely facilitated by MttA, a mitochondrial transporter specific for this intermediate [60, 62]. Notably, aconitase catalyses a reversible reaction that thermodynamically favours CA formation [63].

To eliminate by-products (CA and ICA), the strategy targeted *YlCEX1*, a citrate exporter classified as a plasma membrane drug:H^+ antiporter [56]. Deletion of *YlCEX1* in the IA-producing strain completely suppressed CA and ICA secretion and increased IA titre and yield by 2.8-fold and 3.1-fold, respectively. This deletion also resulted in increased intracellular lipid accumulation (data not shown), likely due to cytosolic CA build-up. This increase may enhance fatty acid synthesis and push the aconitase reaction toward *cis*-aconitate, thereby promoting IA production.

Finally, to enhance IA production, two synthetic pathways – one from *A. terreus* (*cis*-pathway) and one from *U. maydis* (*trans*-pathway) – were combined with the inactivation of both the mitochondrial citrate carrier (YlYhm2) and the plasma membrane citrate exporter (YlCex1). The results revealed a synergistic effect of these genetic modifications, leading to high IA production on glucose (0.303 ± 0.006 mol/mol $Y_{IA/GLU}$) during flask cultivation.

To assess the robustness of this microbial platform for IA production, fed-batch cultivation in 2 L bioreactor was performed using glucose or glycerol as substrates. Pulse-feeding allowed for the achievement of a final IA titre of 55.08 g/L from glucose and 37.71 g/L from glycerol.

To the best of our knowledge, this is the first study where all components of two alternative (*cis* and *trans*) IA biosynthetic pathways were integrated together in a recombinant strain. In the previous studies, where *Y. lipolytica* was used as a microbial factory for IA production at remarkable levels of 54.55 g/L from Waste Cooking Oils (WCO) [47] and 130.50 g/L from glucose [46], the metabolic engineering strategies employed were different. Rong *et al.* (2022) [47] focused on relocating the heterologous IA production pathway to the peroxisomes of *Y. lipolytica* to enhance the conversion of acetyl-CoA – produced via β-oxidation during growth on WCO – into IA. This strategy involved the peroxisomal compartmentalisation of the CadA enzyme from *A. terreus*, overexpression of genes involved in the acetyl-CoA production pathway, and inactivation of competing acetyl-CoA utilisation pathways in peroxisomes. Notably, this approach was effective when using WCO as a substrate but was less applicable to glucose, resulting in a 100-fold lower IA production. In contrast, Fu *et al.* [46] employed a more extensive metabolic engineering strategy. This approach involved preventing carbon accumulation in lipids, relocating IA production to either mitochondria or cytosol, and down-regulating the mitochondrial NAD + -dependent isocitrate dehydrogenase using weak promoters, RNA interference, or CRISPR interference to increase the mitochondrial *cis*-aconitate pool. In their optimised strain, these authors utilised only *cadA* and *mttA* from the *A. terreus* IA biosynthetic pathway as heterologous genes introduced into *Y. lipolytica*. The effect of the heterologous itaconate plasma membrane transporters, MfsA and Itp1, was not tested.

The highest IA production levels in *Y. lipolytica* to date has been obtained by Fu *et al.* [46]. However, it is important to note that scaling up the process with the best-performing recombinant strain required continuous feeding of yeast extract and glucose. This resulted in a nutrient-rich cultivation medium and an extended cultivation period of 24 days.

In contrast to previous studies, the present research focused on a comprehensive reprogramming of both intracellular (overexpression of *mttA* and *mtt1* and deletion of *YlYHM2*) and extracellular (overexpression of *mfsA* and *itp1* and deletion of *YlCEX1*) metabolite transport. These modifications resulted in enhanced IA production and the elimination of side metabolites (CA and ICA) secretion, thereby enhancing the overall yield and selectivity of the process. Unlike previous studies that used nutrient-rich media containing yeast extract, peptone and tryptone [46–48], this study achieved high IA production levels in a minimal medium supplemented only with a carbon source and limiting concentrations of inorganic nitrogen, without requiring additional nutrient supplementation. This approach not only reduces the costs associated with media and substrates but also has the potential to simplify downstream processing.

The yield and the productivity obtained when growing the recombinant strain of *Y. lipolytica* on glucose are the

highest reported to date for any recombinant yeast, being 0.343 mol IA/mol glucose and 0.256 g/L/h, respectively. Furthermore, productivity showed a clear increasing trend over time, stabilising at about 0.4 g/L/h after 161 h. Importantly, no typical by-products of *Y. lipolytica*, such as CA and ICA, were detected in the cultivation medium. The only by-product observed in bioreactors but not in shake-flask cultivations, was a minor amount of succinate, indicating high process selectivity. Specifically, the yield and productivity on glucose were 7% and 13% higher, respectively, compared to the previous best results reported by Fu *et al.* [46].

Conclusions

This study demonstrates that metabolic flux modulation by genetic manipulation of native and heterologous transporters from *A. terreus* and *U. maydis* enhances IA production in *Y. lipolytica*. Introduction of the *A. terreus* pathway genes resulted in low IA production with poor selectivity due to co-secretion of CA and ICA. Targeted deletion of the citrate transporter at mitochondrial (*YlYHM2*) and plasma membrane (*YlCEX1*) levels significantly improved IA yield and selectivity, eliminating by-product secretion into the medium.

Further pathway diversification was explored by integrating the *U. maydis* biosynthetic pathway genes. However, in a wild-type background, IA production remained low, with CA and ICA as major by-products. The selectivity of the process was improved when mitochondrial and plasma membrane citrate transporters were inactivated, although titres remained low. The combination of both biosynthetic pathways, together with the deletion of *YlYHM2* and *YlCEX1*, resulted in strain YM4B493, which achieved the highest IA titre and selectivity among the recombinant strains.

The scalability of this approach was validated in a fed-batch bioprocess where co-feeding of carbon and nitrogen sources resulted in the highest yield and productivity reported for a recombinant *Y. lipolytica* strain using glucose as carbon source. These results highlight the effectiveness of transporter engineering and pathway diversification in optimising microbial IA biosynthesis, paving the way for industrial applications.

Supplementary Information

The online version contains supplementary material available at https://doi.org/10.1186/s13068-025-02668-9.

Supplementary Material 1

Acknowledgements
This research was supported by the University of Bari Aldo Moro. This publication is based upon work from COST Action CA18229 "Yeast4Bio – Non Conventional Yeasts for the Production of Bioproducts", supported by COST (European Cooperation in Science and Technology); www.cost.eu. The authors gratefully acknowledge Nina Filimonova for technical assistance.

Author contributions
C.C.: Conceptualization, Methodology, Investigation, Validation, Writing—Original draft preparation, Writing—Review and Editing. Z.L.: Conceptualization, Writing—Review and Editing. KS: Investigation. E.Y.: Validation, Writing—Review and Editing. T.Y.: Validation, Writing—Review and Editing. I.L.: Investigation, Validation, Writing—Review and Editing. L.P.: Supervision, Funding acquisition. I.P.: Conceptualization, Methodology, Investigation, Validation, Project administration, Writing—Original draft preparation, Supervision. G.A.: Conceptualization, Methodology, Investigation, Validation, Project administration, Writing—Original draft preparation, Supervision.

Funding
This work was financially supported by the National Recovery and Resilience Plan (NRRP), Mission 4. Component 2 Investment 1.5 – Call for proposals POC of 7 November 2023 of Italian Ministry of University and Research funded by the European Union – NextGenerationEU; Award Number: Project code ECS_00000037, CUP H43C22000550001—Spoke 1 Concession Decree No. 2890 of 22 July 2024 adopted by the Italian Ministry of University and Research, Project title "CirBioCas4Urb: Towards a Circular Bioeconomy: Cascading Biotechnological Valorization of Urban Organic Waste for the Production of Bio-Based Products from Volatile Fatty Acids". This work was also partially supported by the CIB ex D.M.n.1059 project "L'innovazione delle Biotecnologie nell'Era della Medicina di Precisione, dei Cambiamenti climatici e dell'Economia Circolare" CUP E93C22003310001 funded by the Italian Ministry of University and Research.

Availability of data and materials
Data is provided within the manuscript or supplementary information files.

Declarations

Ethics approval and consent to participate
Not applicable.

Consent for publication
Not applicable.

Competing interests
The authors declare no competing interests.

Author details
[1]Department of Biosciences, Biotechnologies and Environment, University of Bari Aldo Moro, Campus Universitario, Via Orabona 4, 70125 Bari, Italy. [2]Department of Biotechnology and Food Microbiology, Faculty of Biotechnology and Food Science, Wrocław University of Environmental and Life Sciences, Chelmonskiego 37, 51-630 Wrocław, Poland. [3]Both Strands Ltd, St Albans, Hertfordshire AL1 4QW, UK. [4]Plant Sciences and the Bioeconomy, Rothamsted Research, Harpenden AL5 2JQ, UK. [5]Alterhof LLC, Melnikova 3, Moscow 109316, Russian Federation. [6]Interuniversity Consortium for Biotechnology (CIB), 34100 Trieste, Italy.

Received: 19 March 2025 Accepted: 2 June 2025
Published online: 19 June 2025

References

1. Geilen FMA, Engendahl B, Harwardt A, Marquardt W, Klankermayer J, Leitner W. Selective and flexible transformation of biomass-derived platform chemicals by a multifunctional catalytic system. Angew Chem Int Ed Engl. 2010;49(32):5510–4. https://doi.org/10.1002/anie.201002060.

2. Medway AM, Sperry J. Heterocycle construction using the biomass-derived building block itaconic acid. Green Chem. 2014;16(4):2084–101. https://doi.org/10.1039/C4GC00014E.
3. T. Werpy, G. Petersen, Top Value Added Chemicals from Biomass: Volume I -- Results of Screening for Potential Candidates from Sugars and Synthesis Gas, National Renewable Energy Lab. (NREL), Golden, CO (United States), DOE/GO-102004–1992, 2004. https://doi.org/10.2172/15008859.
4. Market Research Intellect, «Bio-based Itaconic Acid Market Size By Product, By Application, By Geography, Competitive Landscape And Forecast», 923480, 2025. [Online]. Disponibile su: https://www.marketresearchintellect.com/product/global-bio-based-itaconic-acid-market/
5. Verified Market Reports, Global Itaconic Acid Market Size By Derivative (Styrene Butadiene Itaconic Acid, Methyl Methacrylate, Polyitaconic Acid), By Application (SBR Latex, Synthetic Latex, Chillant Dispersant Agent), By Geographic Scope And Forecast», 26175, 2024. [Online]. Disponibile su: https://www.verifiedmarketresearch.com/product/itaconic-acid-market/
6. Robert T, Friebel S. Itaconic acid—a versatile building block for renewable polyesters with enhanced functionality. Green Chem. 2016;18(10):2922–34. https://doi.org/10.1039/C6GC00605A.
7. Teleky B-E, Vodnar DC. Biomass-derived production of itaconic acid as a building block in specialty polymers. Polymers. 2019. https://doi.org/10.3390/polym11061035.
8. Al-Sabagh AM, Sabaa MW, Saad GR, Khidr TT, Khalil TM. Synthesis of polymeric additives based on itaconic acid and their evaluation as pour point depressants for lube oil in relation to rheological flow properties. Egypt J Pet. 2012;21(1):19–30. https://doi.org/10.1016/j.ejpe.2012.02.003.
9. Ji H, et al. Preparation of bio-based elastomer and its nanocomposites based on dimethyl itaconate with versatile properties. Compos Part B Eng. 2023;248:110383. https://doi.org/10.1016/j.compositesb.2022.110383.
10. Zhang Y, et al. Synthesis of bio-based epoxy resins derived from itaconic acid and application in rubber wood surface coating. Ind Crops Prod. 2024;222:119529. https://doi.org/10.1016/j.indcrop.2024.119529.
11. Guo B, et al. Biobased poly(propylene sebacate) as shape memory polymer with tunable switching temperature for potential biomedical applications. Biomacromol. 2011;12(4):1312–21. https://doi.org/10.1021/bm2000378.
12. Brännström S, Malmström E, Johansson M. Biobased UV-curable coatings based on itaconic acid. J Coat Technol Res. 2017;14(4):851–61. https://doi.org/10.1007/s11998-017-9949-y.
13. Kwon YR, Kim HC, Kim JS, Chang Y-W, Park H, Kim DH. Itaconic-acid-based superabsorbent polymer with high gel strength and biocompatibility. Polym Int. 2022;71(9):1090–8. https://doi.org/10.1002/pi.6367.
14. Liu Y, et al. A type of itaconic acid modified polyacrylate with good mechanical performance and biocompatibility. React Funct Polym. 2019;143:104320. https://doi.org/10.1016/j.reactfunctpolym.2019.104320.
15. Bajpai SK, Jyotishi P, Bajpai M. Synthesis of nanosilver loaded chitosan/poly(acrylamide-co-itaconic acid) based inter-polyelectrolyte complex films for antimicrobial applications. Carbohydr Polym. 2016;154:223–30. https://doi.org/10.1016/j.carbpol.2016.08.044.
16. Boschert D, Schneider-Chaabane A, Himmelsbach A, Eickenscheidt A, Lienkamp K. Synthesis and bioactivity of polymer-based synthetic mimics of antimicrobial peptides (SMAMPs) made from asymmetrically disubstituted itaconates. Chem Eur J. 2018;24(32):8217–27. https://doi.org/10.1002/chem.201800907.
17. Michelucci A, et al. Immune-responsive gene 1 protein links metabolism to immunity by catalyzing itaconic acid production. Proc Natl Acad Sci USA. 2013;110(19):7820–5. https://doi.org/10.1073/pnas.1218599110.
18. Mills EL, et al. Itaconate is an anti-inflammatory metabolite that activates Nrf2 via alkylation of KEAP1. Nature. 2018;556(7699):113–7. https://doi.org/10.1038/nature25986.
19. Strelko CL, et al. Itaconic acid is a mammalian metabolite induced during macrophage activation. J Am Chem Soc. 2011;133(41):16386–9. https://doi.org/10.1021/ja2070889.
20. Baup S. Ueber eine neue Pyrogen-Citronensäure, und über Benennung der Pyrogen-Säuren überhaupt. Ann Pharm. 1836;19(1):29–38. https://doi.org/10.1002/jlac.18360190107.
21. da Cruz JC, Camporese Sérvulo EF, de Castro AM, Chapter 10 - Microbial Production of Itaconic Acid, In: Microbial Production of Food Ingredients and Additives, A. M. Holban e A. M. Grumezescu, A c. di, in Handbook of Food Bioengineering. , Academic Press, 2017, pp. 291–316. https://doi.org/10.1016/B978-0-12-811520-6.00010-6.
22. Hegde K, Prabhu A, Sarma SJ, Brar SK, Venkata Dasu V, Chapter 10 - Potential Applications of Renewable Itaconic Acid for the Synthesis of 3-Methyltetrahydrofuran, In: *Platform Chemical Biorefinery*, S. Kaur Brar, S. Jyoti Sarma, e K. Pakshirajan, A c. di, Amsterdam: Elsevier, 2016, pp. 181–200. https://doi.org/10.1016/B978-0-12-802980-0.00010-9.
23. Krull S, Hevekerl A, Kuenz A, Prüße U. Process development of itaconic acid production by a natural wild type strain of *Aspergillus terreus* to reach industrially relevant final titers. Appl Microbiol Biotechnol. 2017;101:10. https://doi.org/10.1007/s00253-017-8192-x.
24. Gopaliya D, Kumar V, Khare SK. Recent advances in itaconic acid production from microbial cell factories. Biocatal Agric Biotechnol. 2021. https://doi.org/10.1016/j.bcab.2021.102130.
25. Steiger MG, Blumhoff ML, Mattanovich D, Sauer M. Biochemistry of microbial itaconic acid production. Front Microbiol. 2013. https://doi.org/10.3389/fmicb.2013.00023.
26. Lass-Flörl C, Dietl A-M, Kontoyiannis DP, Brock M. *Aspergillus terreus* species complex. Clin Microbiol Rev. 2021;34(4):e00311-e320. https://doi.org/10.1128/CMR.00311-20.
27. Thakur R, Shishodia SK, Sharma A, Chauhan A, Kaur S, Shankar J. Accelerating the understanding of *Aspergillus terreus*: Epidemiology, physiology, immunology and advances. Curr Res Microb Sci. 2024;6:100220. https://doi.org/10.1016/j.crmicr.2024.100220.
28. Klement T, Büchs J. Itaconic acid—a biotechnological process in change. Bioresour Technol. 2013;135:422–31. https://doi.org/10.1016/j.biortech.2012.11.141.
29. Okabe M, Lies D, Kanamasa S, Park EY. Biotechnological production of itaconic acid and its biosynthesis in *Aspergillus terreus*. Appl Microbiol Biotechnol. 2009;84(4):597–606. https://doi.org/10.1007/s00253-009-2132-3.
30. Park YS, Itida M, Ohta N, Okabe M. Itaconic acid production using an air-lift bioreactor in repeated batch culture of *Aspergillus terreus*. J Ferment Bioeng. 1994;77(3):329–31. https://doi.org/10.1016/0922-338X(94)90245-3.
31. Tevž G, Benčina M, Legiša M. Enhancing itaconic acid production by *Aspergillus terreus*. Appl Microbiol Biotechnol. 2010;87(5):1657–64. https://doi.org/10.1007/s00253-010-2642-z.
32. Willke Th, Vorlop K-D. Biotechnological production of itaconic acid. Appl Microbiol Biotechnol. 2001;56(3–4):289–95. https://doi.org/10.1007/s002530100685.
33. Geiser E, et al. Ustilago maydis produces itaconic acid via the unusual intermediate trans-aconitate. Microb Biotechnol. 2016;9(1):116–26. https://doi.org/10.1111/1751-7915.12329.
34. Becker J, Tehrani HH, Ernst P, Blank LM, Wierckx N. An optimized ustilago maydis for itaconic acid production at maximal theoretical yield. J Fungi. 2021. https://doi.org/10.3390/jof7010020.
35. Demir HT, et al. High level production of itaconic acid at low pH by Ustilago maydis with fed-batch fermentation. Bioprocess Biosyst Eng. 2021;44:4. https://doi.org/10.1007/s00449-020-02483-6.
36. Hosseinpour Tehrani H, et al. Integrated strain- and process design enable production of 220 g L−1 itaconic acid with *Ustilago maydis*. Biotechnol Biofuels. 2019;12(1):263. https://doi.org/10.1186/s13068-019-1605-6.
37. Ziegler AL, et al. Itaconic acid production by co-feeding of *Ustilago maydis*: a combined approach of experimental data, design of experiments, and metabolic modeling. Biotechnol Bioeng. 2024;121(6):1846–58. https://doi.org/10.1002/bit.28693.
38. Hossain AH, et al. Rewiring a secondary metabolite pathway towards itaconic acid production in *Aspergillus niger*. Microb Cell Factories. 2016;15(1):130. https://doi.org/10.1186/s12934-016-0527-2.
39. Hossain AH, et al. Metabolic engineering with ATP-citrate lyase and nitrogen source supplementation improves itaconic acid production in *Aspergillus niger*. Biotechnol Biofuels. 2019;12(1):233. https://doi.org/10.1186/s13068-019-1577-6.
40. Blazeck J, et al. Metabolic engineering of *Saccharomyces cerevisiae* for itaconic acid production. Appl Microbiol Biotechnol. 2014;98(19):8155–64. https://doi.org/10.1007/s00253-014-5895-0.
41. Otten A, Brocker M, Bott M. Metabolic engineering of *Corynebacterium glutamicum* for the production of itaconate. Metab Eng. 2015;30:156–65. https://doi.org/10.1016/j.ymben.2015.06.003.

42. Chang P, Chen GS, Chu HY, Lu KW, Shen CR. Engineering efficient production of itaconic acid from diverse substrates in *Escherichia coli*. J Biotechnol. 2017;249:73–81. https://doi.org/10.1016/j.jbiotec.2017.03.026.
43. Harder B-J, Bettenbrock K, Klamt S. Model-based metabolic engineering enables high yield itaconic acid production by *Escherichia coli*. Metab Eng. 2016;38:29–37. https://doi.org/10.1016/j.ymben.2016.05.008.
44. Noh MH, Lim HG, Woo SH, Song J, Jung GY. Production of itaconic acid from acetate by engineering acid-tolerant *Escherichia coli* W. Biotechnol Bioeng. 2018;115(3):729–38. https://doi.org/10.1002/bit.26508.
45. Blazeck J, Hill A, Jamoussi M, Pan A, Miller J, Alper HS. Metabolic engineering of *Yarrowia lipolytica* for itaconic acid production. Metab Eng. 2015;32:66–73. https://doi.org/10.1016/j.ymben.2015.09.005.
46. Fu J, et al. Reprogramming *Yarrowia lipolytica* metabolism for efficient synthesis of itaconic acid from flask to semipilot scale. Sci Adv. 2024;10(32):eadn0414. https://doi.org/10.1126/sciadv.adn0414.
47. Rong L, et al. Engineering *Yarrowia lipolytica* to produce itaconic acid from waste cooking oil. Front Bioeng Biotechnol. 2022. https://doi.org/10.3389/fbioe.2022.888869.
48. Zhao C, et al. Enhanced itaconic acid production in *Yarrowia lipolytica* via heterologous expression of a mitochondrial transporter MTT. Appl Microbiol Biotechnol. 2019;103(5):2181–92. https://doi.org/10.1007/s00253-019-09627-z.
49. Larroude M, Rossignol T, Nicaud JM, Ledesma-Amaro R. Synthetic biology tools for engineering *Yarrowia lipolytica*. Biotechnol Adv. 2018;36(8):2150–64. https://doi.org/10.1016/j.biotechadv.2018.10.004.
50. Ledesma-Amaro R, Nicaud JM. Metabolic engineering for expanding the substrate range of *Yarrowia lipolytica*. Trends Biotechnol. 2016;34(10):798–809. https://doi.org/10.1016/j.tibtech.2016.04.010.
51. Wasylenko TM, Ahn WS, Stephanopoulos G. The oxidative pentose phosphate pathway is the primary source of NADPH for lipid overproduction from glucose in *Yarrowia lipolytica*. Metab Eng. 2015;30:27–39. https://doi.org/10.1016/j.ymben.2015.02.007.
52. Yuzbashev TV, et al. A DNA assembly toolkit to unlock the CRISPR/Cas9 potential for metabolic engineering. Commun Biol. 2023;6:1. https://doi.org/10.1038/s42003-023-05202-5.
53. Yuzbasheva EY, et al. The mitochondrial citrate carrier in *Yarrowia lipolytica*: its identification, characterization and functional significance for the production of citric acid. Metab Eng. 2019;54:264–74. https://doi.org/10.1016/j.ymben.2019.05.002.
54. Weber E, Engler C, Gruetzner R, Werner S, Marillonnet S. A modular cloning system for standardized assembly of multigene constructs. PLoS ONE. 2011;6:2. https://doi.org/10.1371/journal.pone.0016765.
55. Yuzbasheva EY, et al. Co-expression of glucose-6-phosphate dehydrogenase and acyl-CoA binding protein enhances lipid accumulation in the yeast *Yarrowia lipolytica*. New Biotechnol. 2017;39:18–21. https://doi.org/10.1016/j.nbt.2017.05.008.
56. Erian AM, Egermeier M, Rassinger A, Marx H, Sauer M. Identification of the citrate exporter Cex1 of *Yarrowia lipolytica*. FEMS Yeast Res. 2020;20:7. https://doi.org/10.1093/femsyr/foaa055.
57. Barth G, Gaillardin C. Yarrowia lipolytica. In: Wolf K, editor. Nonconventional yeasts in biotechnology: a handbook. Berlin, Heidelberg: Springer; 1996. p. 313–88 (**10.1007/978-3-642-79856-6_10**).
58. Chen F, et al. Crystal structure of cis-aconitate decarboxylase reveals the impact of naturally occurring human mutations on itaconate synthesis. Proc Natl Acad Sci USA. 2019;116(41):20644–54. https://doi.org/10.1073/pnas.1908770116.
59. Wierckx N, Agrimi G, Lübeck PS, Steiger MG, Mira NP, Punt PJ. Metabolic specialization in itaconic acid production: a tale of two fungi. Curr Opin Biotechnol. 2020;62:153–9. https://doi.org/10.1016/j.copbio.2019.09.014.
60. Scarcia P, et al. Mitochondrial carriers of *Ustilago maydis* and *Aspergillus terreus* involved in itaconate production: same physiological role but different biochemical features. FEBS Lett. 2020;594(4):728–39. https://doi.org/10.1002/1873-3468.13645.
61. Regev-Rudzki N, Karniely S, Ben-Haim NN, Pines O. Yeast aconitase in two locations and two metabolic pathways: seeing small amounts is believing. Mol Biol Cell. 2005;16(9):4163–71. https://doi.org/10.1091/mbc.e04-11-1028.
62. Steiger MG, Punt PJ, Ram AFJ, Mattanovich D, Sauer M. Characterizing MttA as a mitochondrial cis-aconitic acid transporter by metabolic engineering. Metab Eng. 2016;35:95–104. https://doi.org/10.1016/j.ymben.2016.02.003.
63. Siebert G, Citrate and isocitrate: determination with aconitase and isocitric dehydrogenase, In: Methods of enzymatic analysis, H.-U. Bergmeyer, A c. di, Academic Press, 1965, pp. 318–323. https://doi.org/10.1016/B978-0-12-395630-9.50068-2.

Publisher's Note